J Mater Sci (2010) 45:146–150
DOI 10.1007/s10853-009-3906-9

Temperature-dependent luminescence of gallium-substituted YAG:Ce

Rachael Hansel · Steve Allison · Greg Walker

Received: 6 January 2009 / Accepted: 17 September 2009 / Published online: 30 September 2009

Abstract The temperature-dependent lifetime of trivalent cerium was determined in $(Y_{1-x}Ce_x)_3Al_{2.5}Ga_{2.5}O_{12}$ (where $x = 0.1$ and 0.2) over a temperature range of 20−120 °C. In both samples, the quenching temperature is significantly lower compared to $(Y_{1-x}Ce_x)_3Al_5O_{12}$. The difference in quenching temperatures is explained by evaluating the changes in the lattice, which occur as a result of substituting the Al^{3+} for Ga^{3+}. The information presented in this report is useful for future design of phosphors for use as non-contact temperature sensors.

Introduction

Thermographic phosphors (TGP) are a special class of materials commonly used as non-contact thermometers because their fluorescent decay lifetime is temperature dependent [1]. Cerium-doped yttrium aluminum garnet ($Y_3Al_5O_{12}$:Ce, YAG:Ce) is used in several applications such as solid-state lighting, displays, scintillators, and TGP [1–4]. The Ce^{3+} ion is responsible for nanosecond decay time and an intense yellow-green emission wavelength [5]. Trivalent gallium atoms have been substituted for aluminum in order to blue-shift the emission wavelength for use in solid-state light applications. The excitation and emission of various compositions of gallium-substituted YAG (YAGG) have been extensively studied in recent years. However, there are no studies that identify the temperature-dependence of the luminescent lifetime of Ce^{3+} in YAGG:Ce. In this study, we are interested in the temperature-dependent luminescence of trivalent cerium in gallium-substituted yttrium aluminum garnet (YAGG:Ce).

R. Hansel (✉) · G. Walker
Vanderbilt University, Nashville, TN 37212, USA
e-mail: rachael.a.hansel@vanderbilt.edu

S. Allison
Oak Ridge National Laboratory, P.O. Box 2008, Oak Ridge, TN 37831, USA

Experimental

Samples of $(Y_{1-x}Ce_x)_3Al_{2.5}Ga_{2.5}O_{12}$, where $x = 0.01$ and 0.02, were made by preparing an aqueous solution containing appropriate molar ratios of $Y(NO_3)_3$ (anhy), $Al(NO_3)_3{*}9H_2O$, $Ce(NO_3)_3{*}6H_2O$, and $Ga(NO_3)_3{*}H_2O$. The fuel used to initiate the combustion reaction was urea ($CO(NH_2)_2$) and the oxidant-to-reductant ratio was stoichiometric. Each sample was placed in a muffle furnace at 500 °C to evaporate the water, after which the auto-combustion process began with the evolution of a white gas. Immediately following the auto-combustion, a voluminous, porous yellow powder formed. All samples were calcined for 5 h at 1,000 °C.

The X-ray powder diffraction patterns were measured at room temperature with a Scintag XRD with CuKα ($\lambda = 1.5405$ Å) radiation. Transmission electron microscopy images were taken on a Hitachi 3300 with 300 kV beam. Room temperature photoluminescence measurements were taken using a QuantaMaster-14/2005 with a 150W Xenon lamp excitation source. The emission spectra were recorded using a Quadrascopic monochromator and photomultiplier tube.

The excitation source for the temperature-dependent lifetime experiment was a nitrogen laser (Laser Science Corporation, model VSL-337ND) with $\lambda_{ex} = 337$ nm and an excitation band width of 0.1 nm. The pulse width was 4 ns at a characteristic energy of 300 μJ. The excitation pulse was conveyed via a 1-mm fiber to a 50:50 2 × 1 fiber

optic splitter. The side of the splitter with the single fiber delivers the light to the sample. This same fiber collected and transmitted the emitted signal back through the splitter to a photomultiplier tube, which served as the detector. Each phosphor sample was placed in the bottom of the plastic capsule, which covered the excitation and detector fiber. The capsule/fiber was placed in an oil bath and slowly heated at a rate of 1 °C/min. A k-type bare wire thermocouple (Omega Engineering 871), which was placed near the capsule, monitored the temperature of the phosphor. A bandpass filter centered at 540 nm was used to collect the emitted signal. A waveform processing oscilloscope with 350-Hz bandwidth displayed, digitized, and stored the data.

Results

Structure

The X-ray diffraction (XRD) spectra are shown in Fig. 2 of reference [6]. All samples are highly crystalline and the peaks coincide with the cubic garnet phase of $Y_3Al_5O_{12}$ phase (JCPDS no. 33-40). The presence of gallium in the YAG matrix shifts the peak positions to lower diffraction angles due in part to the fact that the radius of Ga^{3+} is larger than Al^{3+} by about 20.5% in tetrahedral sites and 17% in octaherdral sites [7]. The addition of Ga^{3+} into the YAG structure is influential on the environment of the Ce^{3+}. The Ce^{3+} is coordinated to eight oxygens, which form a distorted cube. This distorted cube is surrounded by four octahedrons and two tetrahedrons, which enclose Al^{3+}. The vertices of the octahedrons and tetrahedrons are oxygen atoms.

When Ga^{3+} is substituted for Al^{3+}, the Ga–O bonds readjust because the atomic radius of Ga^{3+} is larger than Al^{3+}. Ultimately, the substitution of gallium into the YAG lattice results in a decompression of oxygen atoms surrounding the Ce^{3+} atom. As a result, the oxygen atoms directly coordinated to the Ce^{3+} atom become more cubic in structure. This change in structure directly affects the 5d orbitals of the Ce^{3+} and likewise the photoluminescent characteristics.

Photoluminescence

Structural changes induced from the substitution of gallium are readily observed from photoluminescent emission. Emission spectra are shown in reference [6] and a summary of emission data is given in Table 1. Figure 1 shows the relative placement of the 5d orbitals in YAG and YAGG. Electrons are promoted to the E'' state of the 5d orbital and are emitted from the E' state. The splitting, Δ_d, of the E'' and E' states is determined by the crystal field around the Ce^{3+} atom. In unsubstituted YAG, the oxygens around the Ce^{3+} atom are highly compressed and form a distorted cubic structure. The splitting of the E'' and E' states increases as the oxygen atoms are further distorted from the cubic structure. As gallium is substituted into YAG, oxygens surrounding the Ce^{3+} atom are decompressed and form a cubic structure. As a result, the splitting between the E'' and E' states decreases with gallium content. Consequently, the samples with gallium have noticeably lower emission wavelengths (higher energy) and the absorption wavelengths are higher (lower energy). The blue-shifted emission presented in this work correlate well with previous results [8].

Table 1 Structural and spectroscopic properties of $(Y_{1-x}Ce_x)_3(Al_{1-y}Ga_y)_5O_{12}$

x (%Ce)	y (%Ga)	λ_{em} (nm)	Reference
0.01	0	537	[6]
0.01	0.5	514	This work
0.02	0	539	[6]
0.02	0.5	517	This work

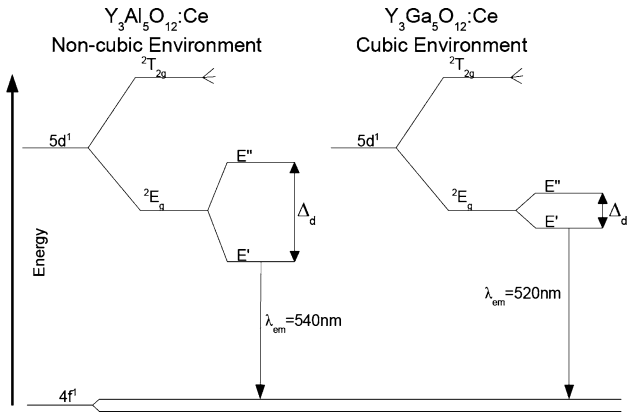

Fig. 1 Energy level diagram for YAG:Ce and YGG:Ce (not drawn to scale)

Transmission electron microscopy

Another important factor, which can significantly influence the photoluminescent properties of YAG:Ce and gallium-substittuted YAG:Ce is the particle morphology. One of the main advantages of combustion synthesis is the ability to rapidly produce highly luminescent crystals from a simple synthesis method. However, it is difficult to obtain uniform particle morphology of the as-synthesized products. Electron microscopy images show that the morphology of each sample varied from large single crystals (Fig. 3) to well-defined nanocrystalline aggregates (Fig. 2). However, the

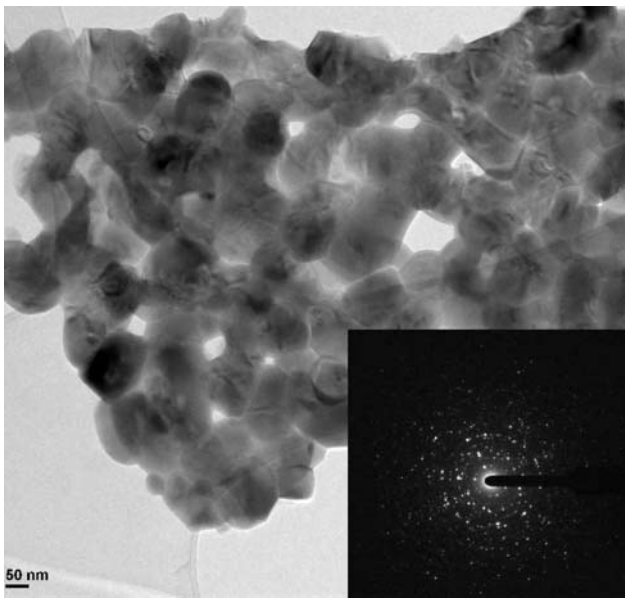

Fig. 2 Bright field image of well-defined nano-crystallites and diffraction pattern

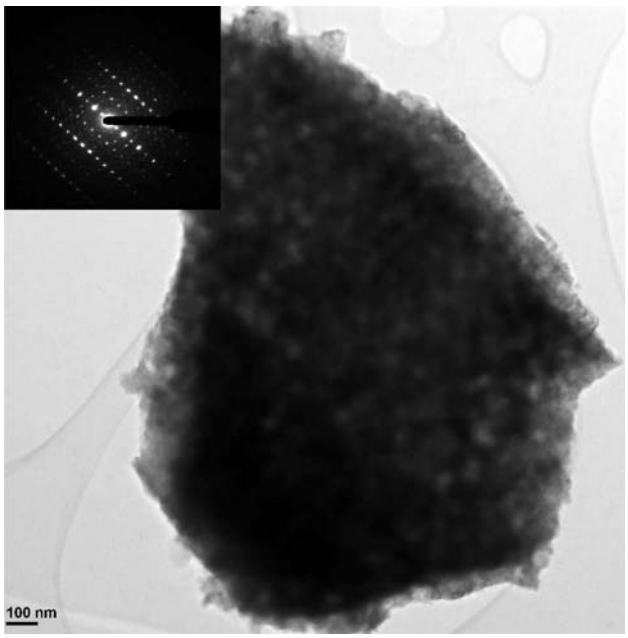

Fig. 3 Bright field image of large single crystal and diffraction pattern

XRD (see Fig. 5) results show that the influence of nano-crystals is not significant since the peaks are very narrow and intense. It has been suggested that nanocrystals can significantly affect the temperature-dependent properties of YAG:Ce [5], however, we will not address the effect of crystal size in this work.

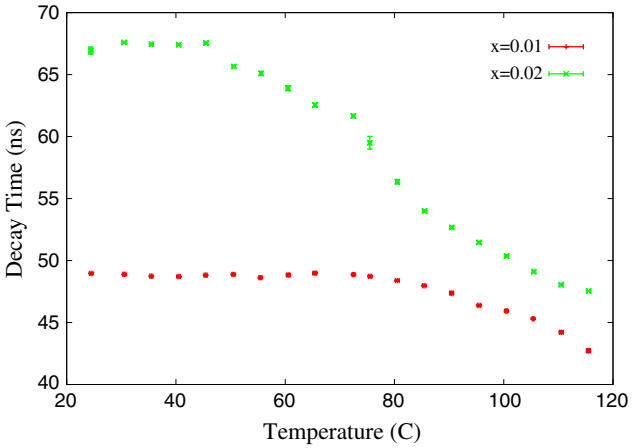

Fig. 4 Decay time versus temperature of $(Y_{1-x}Ce_x)_3Al_{2.5}Ga_{2.5}O_{12}$ using different emission filter

Fluorescence temperature dependency

The goal of this work was to determine the influence of gallium-substitution on the temperature-dependent properties of Ce^{3+} in YAG. To accomplish this goal, the luminescent lifetime as a function of temperature was determined for gallium-substituted garnet phosphors. Plots of the fluorescent lifetime as a function of temperature are shown in Fig. 4. The horizontal error bars represent the error in the temperature (as measured by the thermocouple) which is between 0.15 and 0.33 °C for both samples. The vertical error bars represent the standard deviation in the lifetime measurement and ranged from 0.02 to 0.1 ns for both samples. The lifetime of each sample corresponds well with observed lifetimes in Ce-doped phosphors [4]. The quenching temperature, T_q, is the temperature at which fluorescence begins to decrease due thermal effects within the lattice. For comparison, data from previous work and for commerically-available materials are provided in Table 2.

An increase in the luminescent lifetime is observed when the concentration of Ce^{3+} increases. This effect has been observed before and is due to the reabsorption of emission at higher Ce^{3+} concentrations, which gives rise to longer decay times [9, 10].

Table 2 Quenching temperatures for $(Y_{1-x}Ce_x)_3(Al_{1-y}Ga_y)_5O_{12}$

%Ce	%Ga	T_q (°C)	Reference
1.00	50	90	This work
2.00	50	45	This work
1.00	0	277	[9]
3.33	0	177	[9]
Not reported	0	150	[5]

Discussion

From Fig. 4 and Table 2, it is clear that substituting Ga^{3+} atoms for Al^{3+} in YAG has a profound effect on the luminescent lifetime of Ce^{3+}. The lifetime of the sample with 0.02% cerium is longer than the lifetime of the 0.01% sample because of energy transfer between Ce^{3+} atoms, which results in concentration quenching. Concentration quenching from Ce^{3+} ions is also one reason why the lifetime begins to quench at lower temperatures. However, the goal of this work was to observed how the substitution of Ga^{3+} into YAG alters the quenching of the lifetime. To this end, we have shown that the lifetime of Ce^{3+} begins to quench at much lower temperatures when Ga^{3+} is added to YAG. The reason for this drastic change in quenching temperature is most likely caused by changes in the lattice parameters of the garnet crystal as a result of gallium substitution.

Changes in the lattice parameters are due to the fact that the atomic radius Ga^{3+} is about 20% larger than Al^{3+} in tetrahedral sites (note: Ga^{3+} can substitute in either tetrahedral or octahedral sites. However, Nakatsuka et al. [11] found that Ga^{3+} ions preferentially occupies the tetrahedral sites). Furthermore, the emission wavelength decreases when Ga^{3+} is substituted into the YAG crystal. This blue-shift occurs because the oxygens around the Ce^{3+} atom are forced to form a more cubic structure, which decreases the splitting between the two lowest levels of the 5d orbitals (see Fig. 1).

The energetic position of the two lowest levels of the 5d orbitals can influence non-radiative transitions. Non-radiative transitions are temperature sensitive and are affected by the availability of non-radiative pathways for de-excitation. As the temperature increases, the thermal energy will activate the transfer of energy via a crossover from the lowest vibrational levels of the E' state to high energy vibrational levels of the ground state. Crossover to the ground state will occur at lower temperatures in gallium-substituted garnets because of the decrease in Δ_d, which brings the vibrational levels closer in resonance.

Another factor, which can decrease the quenching temperature of a phosphor, is the size of the particle morphology. Allison et al. [5] have shown that the quenching temperature of nanocrystalline YAG:Ce is as low as 77 °C. Peng et al. [12] have shown that nanocrystals of europium-doped Y_2O_3 exhibit lifetimes, which begin to quench at lower temperatures compared to bulk materials. This decrease in quenching temperature is attributed to the increase in surface-to-volume ratio, which results in an increase in lattice defects. These defects in the lattice serve as traps, which may serve as non-radiative emission pathways [12, 13]. However, our X-ray diffraction results suggest that although aggregated nanocrystals are present in each sample, the majority of the sample is composed of large, micron-sized single crystals. To be sure, we have compared our samples with those of commercially-available micron- and nano-sized phosphors with similar composition (Phosphor Technology and NanoAmor, respectively). From Fig. 5, it is clear that the XRD (in reference to JCPDS no. 33-40) pattern for our sample corresponds almost identically to the bulk sample. Our sample does show some line broadening, which is the result of small crystalline size or non-uniform distortions. However, the peak 2θ values for our sample and bulk sample are nearly identical indicating that the nanocrystalline component of our samples is minimal. Therefore, we attribute the decrease in quenching temperature observed in this work to the addition of Ga^{3+} and not to any size effect.

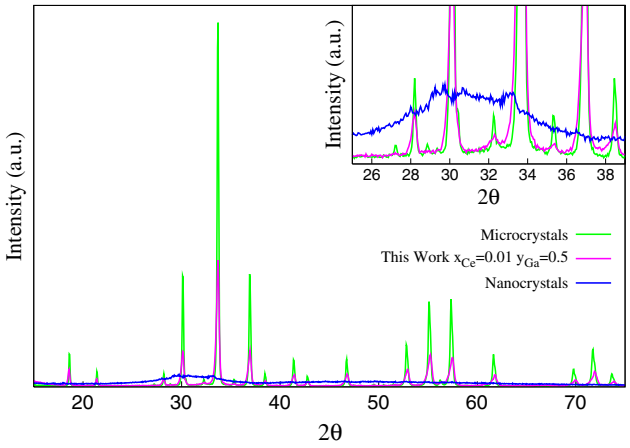

Fig. 5 Comparison of diffraction patterns a sample from the present work with commercially available microcrystals and nanocrystals

Conclusions

The fluorescent lifetime of YAGG:Ce was determined as a function of temperature between 10 and 120 °C. The substitution of Ga^{3+} for Al^{3+} causes the luminescent lifetime of Ce^{3+} to quench at much lower temperatures compared to YAG. The decrease in quenching temperature is attributed to the non-radiative transitions, which can occur as a result of the decrease in splitting of the lowest levels of the 5d orbitals. These results are relevant to the design and implementation of TGP in addition to the development of phosphors used in solid-state lighting, display, or light emitting diodes.

References

1. Allison SW, Gillies GT (1997) Rev Sci Inst 68(7):2615. doi: 10.1063/1.1148174
2. Xia G, Zhou S, Zhang J, Xu J (2005) J Crys Growth 279:357

3. Tous J, Blazek K, Pina L, Sopko B (2007) Radiat Meas 42(4–5): 925. doi:10.1016/j.radmeas.2007.02.040
4. Allison SW, Buczyna JR, Hansel RA, Walker DG, Gillies GT (2009) J App Phys 105(3):036105
5. Allison SW, Gillies GT, Rondinone AJ, Cates MR (2003) Nanotechnology 14:859. doi:10.1088/0957-4484/14/8/304
6. Hansel RA, Allison SW, Walker DG (2008) In: MRS symposium proceedings, vol 1076-K06-06, San Francisco, CA
7. Shannon RD (1976) Acta Cryst A 32:751
8. Wu JL, Gundiah G, Cheetham A (2007) Chem Phys Lett 441:3199. doi:10.1016/j.cplett.2007.05.023
9. Bachmann V, Ronda C, Meijerink A (2009) Chem Mater 21:2077
10. Grinberg M, Sikorska A, Kaczmarek S (2000) J. Alloy Compd 300–301:158
11. Nakatsuka A, Yahiasa A, and Yamanaka T (1999) Acta Crysta B55:266
12. Peng H, Song H, Chen B, Wang J, Lu S, Kong X (2003) J Chem Phys 118(7):3277. doi:10.1063/1.1538181
13. Igarashi T, Ihara M, Kusunoki T, Ohno K, Isobe T, Senna M (2000) Appl Phys Lett 76:1549